Regulation of membrane scission in yeast endocytosis

Deepikaa Menon[1] **and Marko Kaksonen**[1*]

***For correspondence:** Marko.Kaksonen@unige.ch ( )

[1]Department of Biochemistry, University of Geneva, Geneva, Switzerland

Abstract

Introduction

Clathrin-mediated endocytosis (CME) is the major endocytic process by which cargo from the cell exterior is incorporated into a Clathrin-coated vesicle that is then transported into the cell interior (***Bitsikas et al., 2014***). Over 50 different proteins are involved in reshaping a flat plasma membrane into an invagination that eventually forms the vesicle ***Kaksonen and Roux*** (***2018***). Forces that drive the transition from invagination to spherical vesicle in multicellular eukaryotes are provided by the GTPase Dynamin ***Grigliatti et al.*** (***1973***); ***Sweitzer and Hinshaw*** (***1998***); ***Ferguson et al.*** (***2007***); ***Takei et al.*** (***1995***); ***Galli et al.*** (***2017***). Dynamin is now known to interact via its proline-rich-domain with SH3 domains of crescent-shaped N-BAR proteins like Endophilin and Amphiphysin ***Grabs et al.*** (***1997***); ***Cestra et al.*** (***1999***); ***Farsad et al.*** (***2001***); ***Ferguson et al.*** (***2009***); ***Meinecke et al.*** (***2013***). Conformation changes of Dynamin recruited to N-BAR molecules cause constriction of the underlying invaginated membrane, resulting in vesicle formation ***Shupliakov et al.*** (***1997***); ***Zhang and Hinshaw*** (***2001***); ***Zhao et al.*** (***2016***).

In yeast, CME is the only pathway for uptake of cargo, and involves a similar membrane transformation as in other eukaryotes. Most mammalian CME proteins have homologues in yeast: these proteins drive the establishment of endocytic sites, form the mechanical link between membrane and actin proteins ***Kaksonen and Roux*** (***2018***). Actin nucleation and polymerization drives the formation of tubular invaginations in yeast (***Kübler et al., 1993***; ***Kaksonen et al., 2003***). The role of Dynamin in this process has been debated: yeast dynamin-like protein Vps1 has a major role in the Golgi and other membrane trafficking pathways ***Rothman et al.*** (***1990***); ***Peters et al.*** (***2004***); ***Hoepfner et al.*** (***2001***), and been proposed to interact with endocytic proteins ***Nannapaneni et al.*** (***2010***); ***Yu and Cai*** (***2004***); ***Smaczynska-de Rooij et al.*** (***2012***). Its contribution to CME is however, still debated ***Goud Gadila et al.*** (***2017***); ***Kishimoto et al.*** (***2011***). In yeast cells, what causes membrane scission is thus unclear, although the yeast N-BAR Rvs complex (a heterodimeric complex of the proteins Rvs161 and Rvs167) has been identified as an important component of the scission module ***Munn et al.*** (***1995***); ***Kaksonen et al.*** (***2005***); ***D'Hondt et al.*** (***2000***); ***Kishimoto et al.*** (***2011***). The two Rvs proteins are homologues of N-BAR proteins Amphiphysin and Endophilin ***Friesen et al.*** (***2006***); ***Youn et al.*** (***2010***). Deletion of Rvs167 reduces scission efficiency by nearly 30% and reduces the invagination lengths at which scission occurs ***Kaksonen et al.*** (***2005***); ***Kukulski et al.*** (***2012***). Apart from the canonical N-BAR domain which forms the crescent-shaped structure, Rvs167 has a Glycine-Proline-Alanine rich (GPA) region and a C-terminal SH3 domain ***Sivadon et al.*** (***1997***). The GPA region is thought to act as a linker with no other known function, while loss of the SH3 domain affects budding pattern and actin morphology ***Sivadon et al.*** (***1997***). Most Rvs deletion phenotypes

can be rescued by expression of the BAR domains alone ***Sivadon et al.*** (***1997***), suggesting that the BAR domains are the functional unit of the Rvs complex.

The Rvs complex can tubulate liposomes in vitro, indicating that the BAR domains can impose curvature on membranes ***Youn et al.*** (***2010***). However, Rvs arrives at endocytic sites when membrane tubes are already formed: curvature sensing rather than generation is the likely interaction of the complex with endocytic sites ***Kukulski et al.*** (***2012***); ***Picco et al.*** (***2015***). Rvs molecules arrive at endocytic sites about 4 seconds before scission, and disassemble rapidly at the time of scission ***Picco et al.*** (***2015***), consistent with a role in scission. While it is shown to be involved in the last stages of endocytosis, a mechanistic understanding of the influence of Rvs on scission remains incomplete.

Several scission models have been proposed that allow a major role for Rvs and are tested in this work. Although the yeast Dynamin Vps1 lacks a canonical BAR-protein binding site ***Bui et al.*** (***2012***); ***Moustaq et al.*** (***2016***), it may be recruited via a different mechanism and induce scission. Liu et al., proposed that Synaptojanins may selectively hydrolyze lipids at endocytic sites, causing line tension between two lipid types that results in scission ***Liu et al.*** (***2009***). Protein friction along the membrane invagination has been proposed as a mechanism by which scission may occur ***Simunovic et al.*** (***2017***). We used quantitative live-cell imaging and genetic manipulation in Saccharomyces cerevisiae to test these theories and investigate the function of Rvs in endocytosis. We found that Rvs is recruited to endocytic sites by both BAR and SH3 domains. Of several potential actin-interacting binding partners of the SH3 domains such as Myo3, Myo5, Vrp1, Abp1 ***Lila and Drubin*** (***1997***); ***Colwill et al.*** (***1999***); ***Madania et al.*** (***1999***); ***Liu et al.*** (***2009***). we found that type I myosin Myo3 interacts with Rvs SH3 domains. Our data also suggests that the aforementioned theories of membrane scission are unlikely to sever the membrane in yeast, and that actin polymerization likely generates the forces required for scission.

Results

Rvs167, rather than Vps1 influences coat movement

Yeast Dynamin-like protein Vps1 does not contain a Proline Rich Domain, which in mammalian cells is required for recruitment to endocytic sites ***Grabs et al.*** (***1997***); ***Cestra et al.*** (***1999***); ***Farsad et al.*** (***2001***); ***Meinecke et al.*** (***2013***). In spite of the lack of a stereotypical interaction domain, some works have reported its recruitment to endocytic proteins, including to N-BAR protein Rvs167 ***Yu and Cai*** (***2004***); ***Nannapaneni et al.*** (***2010***); ***Rooij et al.*** (***2010***). The question of whether or not Vps1 has a function at endocytic sites has been obfuscated by potential tagging-induced dysfunction of Vps1 molecules. Vps1 tagged both N- and C-terminally with GFP constructs failed to co-localize with endocytic protein Abp1 in our hands, consistent with other work that observed localization only with other parts of the trafficking pathway ***Goud Gadila et al.*** (***2017***). We argued that even if tagging Vps1 induced defects in its localization and/or function, its contribution to endocytosis could be examined by observing the dynamics of other endocytic proteins in cells lacking Vps1. The canonical interaction partner of Vps1- Rvs167- localizes to endocytic sites, and has a role in scission, although it is unclear what that is ***Kukulski et al.*** (***2012***); ***Picco et al.*** (***2015***). In order to determine the roles of these proteins in endocytic scission, we studied cells lacking Vps1 and Rvs167, and compared against wild-type (WT) cells (Fig.1A-F).

Vps1 deletion was confirmed by sequencing the gene locus, and these cells showed a previously reported ***Rothman and Stevens*** (***1986***) growth phenotype at 37°C (Fig.1, supplement1). Scission efficiency was quantified by tracking the endocytic coat protein Sla1 tagged at the C-terminus with eGFP (Fig.1C). Upon actin polymerization, the endocytic coat moves into the cytoplasm along with the membrane as it invaginates ***Skruzny et al.*** (***2012***). Movement of coat protein Sla1 thus acts as a proxy for the growth of the plasma membrane invagination. Membrane retraction, that is, inward

movement and subsequent retraction of the invaginated membrane back towards the cell wall is a scission-specific phenotype ***Kaksonen et al.*** (***2005***). Retraction rates do not significantly increase in *vps1*Δ cells compared to the WT (Fig.1C).

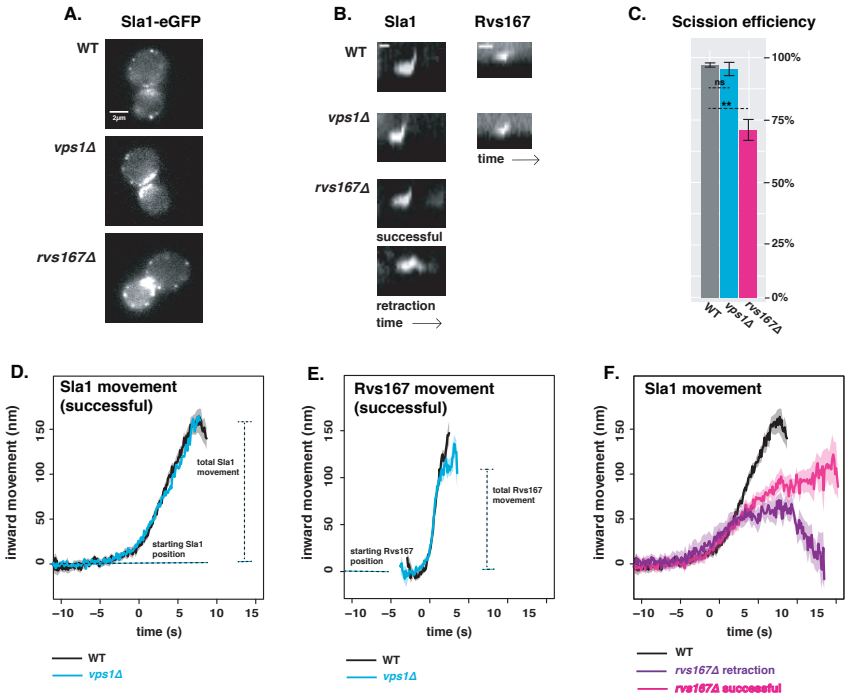

Figure 1. *vps1*Δ and *rvs167*Δ deletion A: Sinlge slices from time lapse movies of WT, *vps1*Δ, and *rvs167*Δ cells expressing Sla1-eGFP. Scale bar= 2μm. **B:** Representative kymographs of Sla1-eGFP and Rvs167-eGFP patches in WT, *vps1*Δ, and *rvs167*Δ cells from time lapse movies. Scale bar for Sla1-egfp = 20(s), scale bar for Rvs167-eGFP = 5(s). **C:** Scission efficiency in WT, *vps1*Δ, and *rvs167*Δ cells. Error bars are standard deviation, p values from t-test, *= p ≤0.05, **= p≤0.01, ***=p≤0.001. **D:** Averaged centroid positions of Sla1-eGFP in WT and *vps1*Δ cells. **E:** Averaged position of Rvs167-eGFP in WT and *vps1*Δ cells.**F:** Averaged position of Sla1-eGFP in WT, and successful and retracted Sla1-eGFP positions in *rvs167*Δ cells. All averaged positions were aligned in x axis to begin inward movement at time=0(s), and aligned in the y axis to a starting position = 0(nm).

The total movement of the endocytic coat (Fig.1D,E) gives an indication of when invagination has undergone scission: greater movement would imply defects in the scission mechanism. In order to study this movement , the averaged centroid trajectory of 50 Sla1-eGFP patches in *vps1*Δ and WT cells were tracked and compared (Fig.1D). In brief: yeast cells expressing fluorescently-tagged endocytic proteins were imaged at the equatorial plane. Since membrane invagination progresses perpendicularly to the plane of the plasma membrane, proteins that move into the cytoplasm during invagination do so in the imaging plane. Centroids of Sla1 patches- each patch being an endocytic site- were tracked in time and averaged. This provided an average centroid that could be followed with high spatial and temporal precision ***Picco et al.*** (***2015***). Averaged centroid movement of Sla1-eGFP in WT cells was linear to about 140nm (Fig.1D). Sla1 movement in *vps1*Δ cells had the same magnitude of movement (Fig.1D). In spite of slight differences in the rates of movement, the total movement- and so the depth of endocytic invagination- did not change.

Centroid tracking has shown that the number of molecules of Rvs167 peaks at the time of scission, and is followed by a rapid loss of fluorescent intensity, simultaneous with a sharp jump of the centroid into the cytoplasm ***Picco et al.*** (***2015***). This jump, also seen in Rvs167-GFP kymographs

(Fig.1B), is interpreted as loss of protein on the membrane tube, causing an apparent spatial jump to the protein localized at the base of the newly formed vesicle. Kymographs of Rvs167-GFP (Fig.1B), as well as Rvs167 centroid tracking (Fig.1E) in Vps1 deleted cells showed the same jump as in WT.

The Rvs complex is composed of Rvs161 and Rvs167 dimers (Boeke et al. 2014) so deletion of Rvs167 effectively removes both proteins from endocytic sites. We quantified the effect of *rvs167*Δ on membrane invagination (Fig.1A-C,F). Only 73% of Sla1 patches undergo successful scission in *rvs167*Δ cells (Fig.1C). Similar scission rates have been measured in other experiments ***Kaksonen et al.*** (***2005***), and suggest failed scission in the remaining 27% of endocytic events. Coat movement both of retractions and of successful endocytic events were quantified (Fig.1F) as described earlier. Sla1 centroid movement in both successful and retracting endocytic events in *rvs167*Δ cells look similar to WT up to about 50nm (Fig.1F). In WT cells, Abp1 intensity begins to drop at scission time (Fig.1supplement2); similarly, in successful endocytic events, Abp1 intensity drops after Sla1 centroid has moved about 100nm suggesting that scission occurs at invagination lengths between 60 -100 nm (Fig,1supplement4). That membrane scission occurs at shorter invagination lengths than in WT is corroborated by the smaller vesicles formed in *rvs167*Δ cells by Correlative light and electron microscopy (CLEM) ***Kukulski et al.*** (***2012***). CLEM has moreover shown that Rvs167 localizes to endocytic sites after the invaginations are about 60nm long ***Kukulski et al.*** (***2012***). Sla1 movement in *rvs167*Δ indicates therefore that membrane invagination is unaffected till Rvs is supposed to arrive.

Synaptojanins likely influence vesicle uncoating, but not scission dynamics.

As Vps1 did not appear to influence membrane scission, we proceeded to test another scission model. The lipid hydrolysis model proposes that deletion of yeast synaptojanins would inhibit scission and therefore result in longer invaginations ***Liu et al.*** (***2009***). Three Synaptojanin-like proteins have been identified in S. cerevisiae: Inp51, Inp52, and Inp53. Inp51-eGFP exhibits a diffuse cytoplasmic signal, Inp52-eGFP localizes to cortical patches that are endocytic sites (Fig.2A, supplement) and Inp53 localizes to patches within the cytoplasm (Fig.2A, ***Bensen et al.*** (***2000***)). Since Inp52 localizes to endocytic sites, we began with determining the spatial and temporal recruitment of Inp52 within the endocytic machinery. We aligned the averaged centroid of Inp52 in space and time to other endocytic proteins ***Picco et al.*** (***2015***). In order to do this, we imaged Inp52-eGFP simultaneously with Abp1-mCherry, and did the same with Sla1-eGFP and Rvs167-eGFP. Using Abp1 as the common reference frame, we were able to compare the arrival of the different proteins with respect to that of Abp1. We assigned as time =0 (s) the fluorescent intensity maximum of Abp1, which in WT cells is concomitant with membrane scission, and also coincides with the maximum of the Rvs167 fluorescent intensity (Fig.1A, supplement2). On the y axis, 0 (nm) indicates the position of the Sla1 centroid; positions of the other centroids are in relation to the Sla1 centroid. Inp52 molecules arrived in the late stage of endocytosis after Rvs167 arrival, and localized to the invagination tip, suggesting a potential role in membrane scission (Fig.2B).

Inp53 was not investigated further, as its localization conformed with other literature that found that it is involved in the golgi trafficking pathway and not endocytosis ***Bensen et al.*** (***2000***). Although we were unable to observe localization of Inp51 at endocytic sites, deletion of Inp51 has been shown to exacerbate the effect of *inp52*Δ on membrane retraction ***Liu et al.*** (***2009***), so both Inp51 and Inp52 were tested as potential scission regulators.

Dynamics of Sla1-eGFP and Rvs167-eGFP in *inp51*Δ and *inp52*Δ cells were compared against the WT (Fig.2C-E). Scission efficiency did not significantly decrease in *inp51*Δ compared to the WT, but showed a slight decrease in *inp52*Δ cells (Fig2C). Total movement of Sla1 and Rvs167 centroids in *inp51*Δ were the same as in WT (Fig.2 D,E), while Rvs167 assembly and disassembly took longer (Fig.2supplement). Rvs167 centroid, after the inward movement, appeared to persist compared to

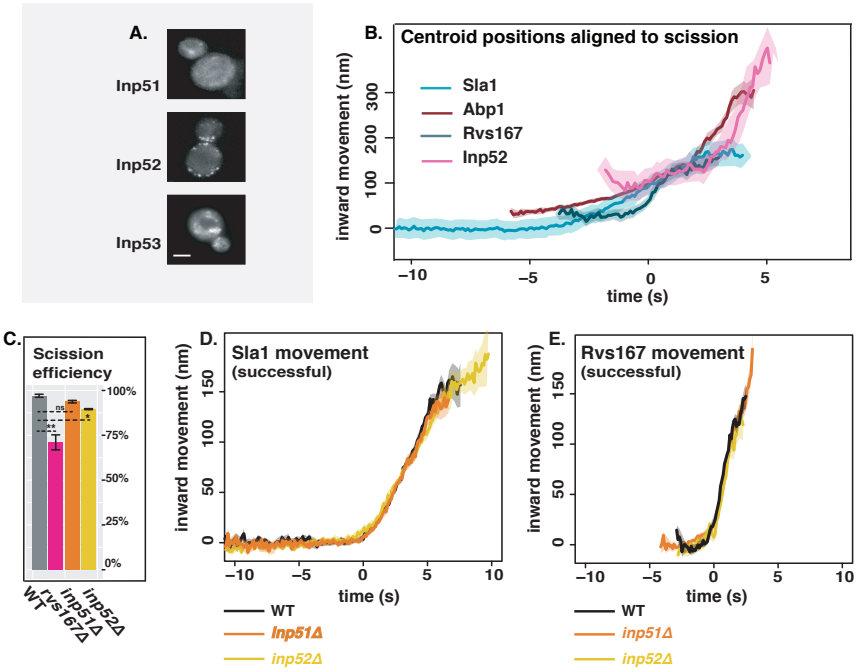

Figure 2. Involvement of yeast Synaptojanin-like proteins in endocytosis **A:** Cells endogenously tagged with Inp51-, Inp52-, and Inp53-eGFP. **B:** Inp52 centroid trajectory was aligned in space and time to other endocytic proteins. **C:** Sla1 retraction rates in *inp51*Δ and *inp52*Δ cells compared to WT and *rvs167*Δ. Error bars are standard deviation, with p values from t-test, *= p≤0.05, **= p≤0.01, ***=p≤0.001. **D:** Averaged centroid positions of Sla1-eGFP in WT, *inp51*Δ, and *inp52*Δ cells. **E:** Averaged centroid positions of Rvs167-eGFP in WT, *inp51*Δ, and *inp52*Δ cells.

the WT, likely because of a delay in Rvs167 disassembly from the newly formed vesicle. In *inp52*Δ cells, Sla1 movement had the same magnitude and rate as in WT, but Sla1-eGFP signal is persistent after inward movement scission (Fig.2D). Rvs167 and Sla1 disassembly were delayed in *inp52*Δ cells compared to WT (Fig.2supplement1). This data are consistent with Synaptojanin involvement in assembly and disassembly of coat and scission proteins at endocytic sites rather than in membrane scission.

Rvs BAR domains recognize membrane curvature in-vivo

So far Rvs167 remains the protein that has a major influence on scission efficiency and movement of Sla1. Rvs can tubulate liposomes in vitro ***Youn et al.*** (***2010***), but its interaction with membrane curvature in vivo has not so far been tested. Recruitment of the Rvs complex to endocytic sites, and BAR-membrane interaction was thus investigated further. The SH3 domain has known interactions with proteins within actin network ***Lila and Drubin*** (***1997***); ***Colwill et al.*** (***1999***); ***Madania et al.*** (***1999***); ***Liu et al.*** (***2009***). We removed the contribution of the SH3 by deleting the domain (Fig.3A) and observed the localization of Rvs167Δ*sh3* compared to full-length Rvs167. Endogenously tagged Rvs167-eGFP and Rvs167Δ*sh3*-eGFP colocalization with Abp1-mCherry in WT and *sla2*Δ cells were compared (Fig.3B). Sla2 acts as the molecular linker between forces exerted by the actin network and the plasma membrane ***Skruzny et al.*** (***2012***). *sla2*Δ cells therefore contain a polymerizing actin network at endocytic patches, but the membrane has no curvature, and endocytosis fails. In these cells, the full-length Rvs167 co-localizes with Abp1-mCherry, indicating that it is recruited to endocytic sites independently of membrane curvature (Fig.3B, "*sla2*Δ"). Rvs167Δ*sh3* does not localize to the plasma membrane except for rare transient patches that do not co-localize with Abp1-mCherry: Rvs167Δ*sh3* is not recruited to endocytic sites in the absence of curvature in *sla2*Δ cells.

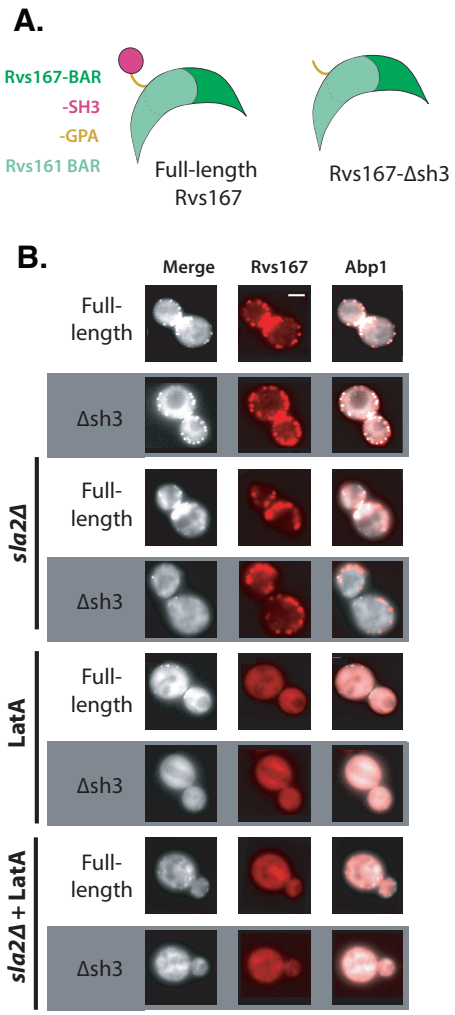

Figure 3. Localization of Rvs167 BAR domain A: Schematic of Rvs protein complex with and without the SH3 domain. **B:** Localization of full-length Rvs167 and Rvs167Δ*sh3* in WT, *sla2*Δ, LatA treated, and LatA treated *sla2*Δ cells. Scale bar=2μm.

Rvs SH3 domains have an actin and curvature independent localisation

In order to test if genetic interactions of SH3 domains are prevalent in in vivo endocyotosis, we tested the localization of Rvs167 and Rvs167textitΔsh3 in LatA treated cells (Fig.3B, "LatA"). Plasma membrane localization of Rvs167 remains upon LatA treatment, and transient patches continue to exist in *sla2*Δ cells treated with LatA (Fig3B, "*sla2*Δ+ LatA"). Rvs167textitΔsh3 does not localize to the plasma membrane in either case. Thus, localization of full-length Rvs167 in the presence of LatA is due to the SH3 domain. This indicates that the SH3 domain is able to recruit Rvs molecules to the plasma membrane in an actin- and curvature-independent manner.

SH3 domains are likely recruited by Myosin 3

Type I myosins Myo3 and Myo5, and Vrp1 have known genetic and/or physical interactions with Rvs167 SH3 domains ***Lila and Drubin*** (***1997***); ***Colwill et al.*** (***1999***); ***Madania et al.*** (***1999***); ***Liu et al.*** (***2009***). We tested the interaction between these proteins and the Rvs167 SH3 region by studying the localization of full-length Rvs167 in cells with one of the genes for these proteins deleted, and treated with LatA. By using LatA we expected to reproduce the situation in which BAR-curvature interaction is removed (Fig.4B). Then, if we lost SH3 interaction because we removed the protein

with which it interacts, we would lose localization of Rvs167 completely. Deletion of neither Vrp1 nor Myo5 in combination with LatA treatment removes the localization of Rvs167. Deletion of Myo3 with LatA treatment removes localization of Rvs167, indicating that SH3 domains interact at endocytic sites with Myo3.

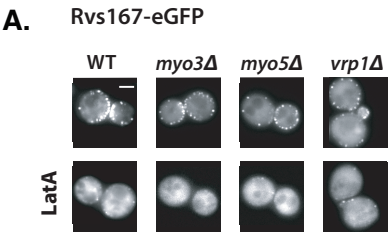

Figure 4. Localization of the SH3 domain Localization of full-length Rvs167-eGFP in WT, *myo3*Δ, *myo5*Δ, and *vrp1*Δ cells. Scale bars=2μm.

what about the differences in myo5 and myo3 number...

Loss of Rvs167 SH3 domain affects coat and actin dynamics

Since the Rvs167 SH3 domain has an influence on the recruitment of the Rvs complex to endocytic sites, we wondered if the domain also affects later stages of invagination formation endocytic dynamics. We compared dynamics of coat and scission markers in WT and *rvs167*Δ*sh3* cells (Fig.5). Movement of Sla1 centroid is slower and reduced in *rvs167*Δ*sh3* cells compared to WT (Fig4A,B). The movement of Rvs167textitΔsh3 centroid is smaller than that of full-length Rvs167 (Fig.5A,B), consistent with the formation of shorter invaginations suggested by the reduced Sla1 movement in *rvs167*Δ*sh3* cells.

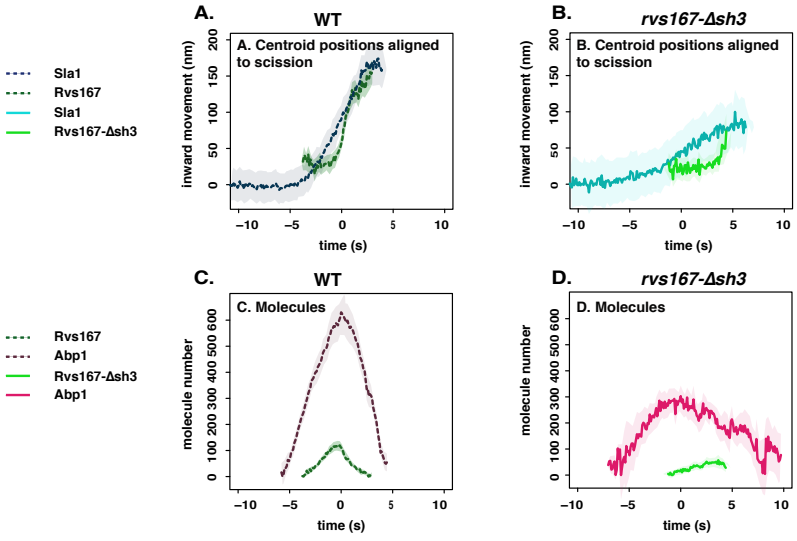

Figure 5. Endocytic dynamics in BAR-GPA cells A,B: Averaged centroid positions aligned in x axis so that time=0(s) is the peak of fluorescent intensity of Abp1 in respective strains. Centroids are aligned in y axis so that Sla1 begins at y=0 (nm), and Rvs167 and Rvs167Δ*sh3* positions are determined with respect to Sla1 centoids. **C,D:** Numbers of molecules of in WT and *rvs167*Δ*sh3* cells, aligned so that time=0(s) is the maximum of fluorescent intensity of Abp1 in the corresponding strains.

There is delay in Rvs167Δ*sh3* recruitment compared to the onset of Abp1 assembly in *rvs167*Δ*sh3* cells compared to WT (Fig.5 C,D). In WT cells, Rvs167 and Abp1 molecule number peaks are also co-

incident: the actin network begins disassembling as soon as scission occurs (Fig.5C). Asynchronous peaks in *rvs167*Δ*sh3* cells indicates a disruption in the feedback between actin network dynamics and membrane scission. Rvs167textitΔsh3 accumulation begins however, when Abp1 molecule numbers in the mutant are about the same as in WT (about 300 copies, Fig.5C,D). . Both Rvs167 and Rvs167Δ*sh3* molecules arrive at endocytic sites when the Sla1 centroid is 20-30 nm away from its starting position. This would mean the endocytic coat has moved about 30 nm when both WT and mutant forms of Rvs are recruited. That Rvs167Δ*sh3* recruitment anticipates a certain growth of the invagination and amount of Abp1 suggests that the Rvs complex is recruited to a specific geometry of membrane invagination, and that Rvs167Δ*sh3* recruitment is delayed because invaginations in these cells take longer to acquire this specific geometry. Recruitment of Rvs167Δ*sh3* is reduced to half of Rvs167 (Fig.5C,D), although cytoplasmic concentration of both are similar (Fig.5supplement1). Recruitment therefore is unlikely to be limited by cytoplasmic expression of the mutant protein. Abp1 disassembly is slowed down in *rvs167*Δ*sh3* cells compared to WT, and recruitment is reduced to 50% of WT recruitment (Fig.5C,D), indicating disruption of actin network dynamics.

Increased BAR domain recruitment corresponds to increased membrane movement

Since removal of Rvs167 in *rvs167*Δ*sh3* cells, and the reduced amount of Rvs167Δ*sh3* recruited in *rvs167*Δ*sh3* cells results in decreased Sla1 movement, we wondered if Sla1 movement would scale with amount of Rvs recruited to endocytic sites. We titrated the amount of Rvs expressed in cells by endogenously duplicating the Rvs167 and Rvs161 genes (Huber et al. 2014) in diploid and haploid yeast cells (Fig.5) . We thus made diploid strains with 4x copies of both the Rvs genes (4xRVS), 2x copies (WT diploid cells, 2xRVS), and 1x copy (1xRVS). Number of molecules of Rvs167 recruited to endocytic sites increases with gene copy number (Fig5A). “Excess” Rvs recruited to endocytic sites in the 4xRVS case does not change the rate or total movement of Sla1, or of Rvs167 (Fig.6B,C) compared to the WT (2xRVS). In the case of 1xRVS, Sla1 movement is slightly reduced after 100nm (Fig5B). Magnitude of Rvs167 inward movement was similar in all three, but the Rvs167-eGFP signal was lost immediately after the inward movement in the 1xRVS case, unlike in the 4xRVS and 2xRVS cases, likely because fewer molecules are recruited (Fig.6A). Unlike in the *rvs167*Δ*sh3* case, Abp1 and Rvs167 peaks were concomitant in all three strains, with similar amounts of Abp1 recruited irrespective of Rvs gene copies (Fig.6D). Thus was there no apparent disruption of the actin network, or of the coupling between scission and actin network disassembly. Adding more Rvs than in the WT diploid case did not lead to differences in Sla1 movement, although reducing the amount of Rvs- as in the 1xRVS case- marginally decreased movement.

In haploid cells, we duplicated the full-length Rvs167 gene, as well as *rvs167*Δ*sh3* gene (Fig5E-H). We thus produced strains with 2x copies of the Rvs genes (2xRVS), 1x copy of each (WT haploid, 1xRVS), 2x copies of the *rvs167*Δ*sh3* gene (2xBAR), or 1 copy of *rvs167*Δ*sh3* gene (1xBAR). Amount of WT and mutant Rvs167 molecules recruited at endocytic sites varied in these strains between 50 and 180 copies (Fig5E). Sla1 dynamics remained the same in Rvs duplicated strain (2xRVS) as in the WT (Fig.6F). In the 2xBAR case, the amount of Rvs167Δ*sh3* molecules recruited to endocytic sites increased (Fig.6E), as did Sla1 movement, as well the inward jump of Rvs167 (Fig.6F,G), compared to 1xBAR. Total Abp1 numbers recruited were reduced in 1xBAR (that is *rvs167*Δ*sh3*), compared to the 2xBAR, 1xRVS and 2xRVS (Fig5H). Higher Abp1 numbers corresponds to larger Sla1 centroid movement in both diploid and haploid cells (Fig.6C, D, G, H), suggesting a correlation between the maximum number of Abp1 recruited and total invagination length.

Discussion

Recruitment and function of the Rvs complex in has been explored in this work, as well as several models for how membrane scission could be effected in yeast endocytosis. We propose that Rvs is recruited to endocytic sites by interactions between the Rvs BAR domains and invaginated

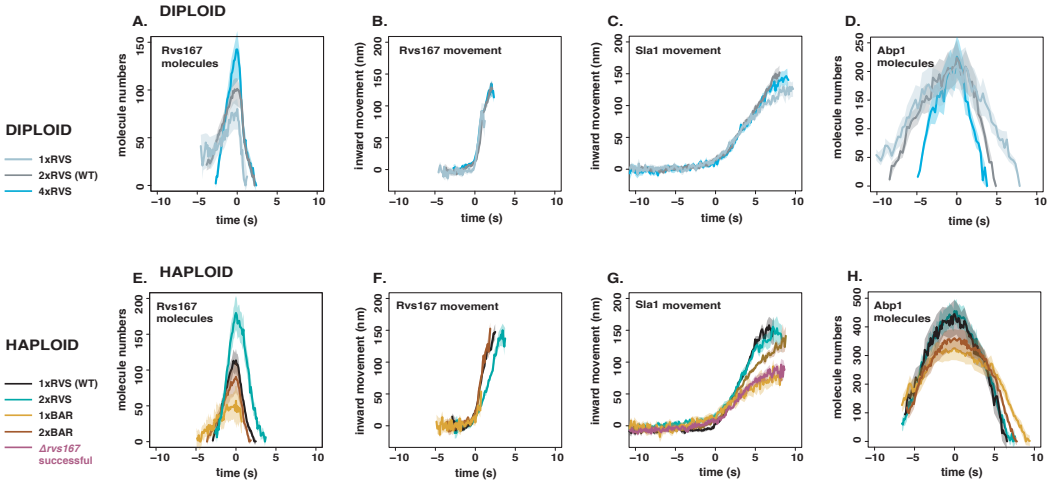

Figure 6. RVS duplication in haploid and diploid cells A: Recruitment of Rvs167 in diploid strains with different copy number of Rvs167 and Rvs161 genes. **B:** Rvs167 centroid positions in these strains **C:** Sla1 centroid positions in these strains. **D:** Abp1 molecule numbers in same strains, with only one Abp1 allele tagged. **E,F:** Recruitment and centroid positions of Rvs167 and Rvs167Δ*sh3* in haploid strains. **G:** Sla1 centroid positions in these strains. **H:** Abp1 recruitment in the same strains. All centroid positions were aligned in the time axis so that time=0(s) corresponds to beginning of inward movement of each average centroid. Centroids were aligned in the y axis so that y=0(nm) corresponds to the beginning of the average centroid position

membrane, and that SH3 domain mediated protein-protein interactions are required for efficient recruitment of Rvs to sites. Arrival of Rvs on membrane tube scaffolds the membrane and prevents premature membrane scission. Effective scaffolding depends on recruitment of a critical number of Rvs molecules. Rvs is a relatively short-lived protein at endocytic sites. It is recruited only once membrane tube is formed (Kaksonen, Toret and Drubin, 2005; Kukulski et al., 2012; Picco et al., 2015). FCS measurements (Boeke et al., 2014) have shown that the cytosolic concentrations of Rvs167 and Rvs161 are high (354nM and 721nM respectively) compared to other endocytic proteins like Las17, Vrp1, Myo3, and Myo5 (80-240nM). In spite of this, relatively few numbers of Rvs are recruited to endocytic sites, suggesting that recruitment is tightly regulated. In the case of Rvs, both timing and efficiency appear crucial to its function, the question is what confers both.

BAR domains sense *in vivo* membrane curvature and time recruitment of Rvs

The curved structure of BAR dimers (Peter et al., 2004; Mim et al., 2012) has suggested that Rvs is recruited by its preference for some membrane shapes over others, supported by its arrival at curved membrane tubes. In the absence of membrane curvature, in *sla2*Δ cells, the BAR domain alone does not localize to cortical patches (Fig.3b,c). This demonstrates for the first time that the BAR domain does indeed sense and requires membrane curvature to localize to cortical patches. Work on BAR domains have proposed that electrostatic interactions at the concave surface and tips of the BAR domain structure mediate membrane binding (Qualmann, Koch and Kessels, 2011). Mutations in these lipid-binding surfaces would clarify the interaction with underlying lipids, and test if Rvs relies on similar interactions. BAR is able to localize to endocytic sites, and has a similar lifetime in WT cells (Fig4b). However, time alignment with Abp1 shows that there is a delay in the recruitment of BAR-GPA compared to Abp1 arrival, compared to full-length Rvd167 (Fig4c). The delayed recruitment occurs because the invagination takes longer to reach a particular length: Sla1 moves inwards at a slower rate in BAR cells, and it takes longer for the membrane in BAR-GPA cells to reach the same length as Rvs167. Rvs167 arrives in BAR cells when Sla1 has moved inwards 25-30nm (dashed red lines in Fig.4a), which is also the distance Sla1 has moved when Rvs167 arrives in WT. By the time Sla1 has moved this distance, the membrane is already tubular (Kukulski et

al., 2012; Picco et al., 2015), consistent with Rvs arrival at invaginated tubes. This suggests Rvs recruitment is timed to specific membrane invagination length- therefore to a specific membrane curvature- and that this timing is provided by the BAR domain.

SH3 domains allow efficient and actin independent recruitment

Rvs167 in BAR cells accumulates to about half the WT number (Fig.3c), even though the same cytoplasmic concentration is measured (supplement Fig3?), indicating that the SH3 domain increases the efficiency of recruitment of Rvs. In *sla2*Δ cells, full-length Rvs can assemble on the membrane (Fig.3b,c). Since BAR domains alone do not localize to patches in *sla2*Δ cells, full-length localization must be mediated by the SH3 domain, supporting a role for the SH3 domain in increasing recruitment of Rvs by clustering protein molecules. That full-length Rvs167 is able to assemble and disassemble at cortical patches in *sla2*Δ cells without the curvature- dependent interaction of the BAR domain (Fig.3b,c) indicates that the SH3 domain is able to mediate both the recruitment and the disassembly of Rvs at the endocytic site. In *sla2*Δ cells treated with LatA (Fig.3c), actin-based membrane curvature is inhibited, and the actin patch proteins are removed from the plasma membrane. Full-length Rvs167 in these cells still shows transient localizations at the plasma membrane. In *sla2*Δ cells treated with LatA, the localization of BAR is lost. This suggests that localization of the full-length Rvs167 in LatA treated cells is dependent on an SH3 domain interaction, and that this is independent of both actin and membrane curvature.

In WT cells, the Abp1 and Rvs167 fluorescent intensities reach maxima concomitantly (Fig4b), and the consequent decay of both also coincide. Coincident disassembly indicates that upon vesicle scission, the actin network is immediately disassembled. Membrane scission essentially occurs around the intensity peak of the two proteins. This coincident peak is lost in BAR-GPA cells: BAR-GPA-eGFP in these cells peaks several seconds after Abp1 intensity starts to drop, and the decay of Abp1 is prolonged, taking nearly double the time as in WT. The number of Abp1 molecules recruited is decreased to about two thirds the WT number. Although it is not clear what the decoupling of Abp1 and Rvs peaks means, the changes in Abp1 dynamics suggests a strong disruption of the actin network dynamics. SH3 domains are known to interact with components of the actin network like Abp1 and Las17 (Lila and Drubin, 1997, Madania et al., 1999), but study of other components of the actin machinery will be required to understand how exactly loss of the SH3 has changed the progression of endocytosis.

SH3 interaction with an endocytic binding partner likely help recruit Rvs to endocytic sites. Many such interaction partners have been proposed. Abp1 interaction with the Rvs167 SH3 domain has been shown (Lila and Drubin, 1997; Colwill et al., 1999), as has one with WASP protein Las17 (Madania et al., 1999; Liu et al., 2009), yeast Calmodulin Cmd1 (Myers et al., 2016), type I myosins (Geli et al., 2000), and Vrp1 (Lila and Drubin, 1997). All of these suggested binding partners localize to the base of the invagination (Yidi Sun, 2006; Picco et al., 2015), and do not follow the invaginating membrane into the cytoplasm. The SH3 interaction partner is likely Myo3 (Fig3d), and SH3 domains interact with the endocytic network at the base of the invagination. Centroid tracking however, suggests that Rvs is accumulated all over the membrane tube. If Rvs was recruited to the base and pulled up as the invagination grows, the centroid would move continuously upwards rather than remain relatively non-motile before the jump at scission time. It is possible that the SH3 initially helps cluster near the base, and as the membrane invaginations grow longer, BAR-membrane interactions dominate.

Accumulation of Rvs on membrane invagination

When ploidy is doubled from haploid to diploid yeast cells, we could expect that double the protein amount is expressed and recruited, but it does not appear so. The amount of Rvs recruited in WT haploid and diploids remains about the same, and cytoplasmic signal is similar (Fig.5, Fig5 supplement). This invariance between accumulated protein in haploids and diploids shows that Rvs recruitment is not determined by the number of alleles of Rvs. Haploid and diploid cells appear

to tune the amount of Rvs recruitment to get a specific amount to endocytic sites. WT diploids (2xd) contain two copies each of RVS161 and RVS167 genes. Rvs duplicated diploids, which contain four copies each of RVS167 and RVS161 (4xd) could be expected to express and recruit to sites twice the amount of Rvs as 2xd. However, compared to 2xd, cytoplasmic signal in 4xd increases by 1.6x and recruitment of Rvs167 to endocytic sites increases only by 1.4x. Doubling the gene copy number increases, but does not double protein expression or recruitment in the case of Rvs. Similarly, duplicating Rvs genes in haploid cells results in an increase in number of molecules recruited, but not in doubling (1xh, 2xh). Although the rate of adding Rvs is different in haploids and diploids, in both cases, it increases by gene copy number (yellow line in Fig.4.2). Cytoplasmic protein concentration is increased when gene copy num- ber is increased, and recruitment to endocytic sites is increased by the increase in cytoplasmic concentration. These data suggest that the amount of Rvs that is recruited scales with available concentration of protein. Comparing across ploidy however, the rate of Rvs recruitment is lower in WT diploid compared to WT haploid (2xd vs 1xh, Fig.4.1)

for this is not clear. 4.2 Arrangement of Rvs dimers on the mem- brane A homology model of the Rvs BAR dimer structure based on Am- phiphysin suggests that it has the concave structure typical for N- BAR domains. Rvs is a hetero- rather than homodimer unlike Am- phiphysin, and a high-resolution structure will be necessary to clarify the interaction and arrangement of Rvs on endocytic tubes. There are some indications from the experiments in this thesis however, regarding its interaction with the membrane. 4.2.1 Rvs does not form a tight scaffold on membrane tubes Observations of in vitro helices of BAR domains have suggested that Rvs might form a similar helical scaffold. The number of Rvs molecules recruited to endocytic sites is high enough to cover the surface area of the tubular invagination, so it has been proposed that an Rvs scaffold covers the entire membrane tube up to the base of the future vesicle (Picco et al., 2015). In Rvs duplicated diploid cells (4xd), Rvs can be recruited at a much faster rate than in the WT (2xd) (Fig.3.10B-C, Fig.4.2) while disassembly dynamics is the same in both (Fig.3.10C, Fig.4.3). The exponential decay of fluorescent intensity in WT haploid and diploid cells (1xh, 2xd, Fig.4.3) indicates that all of the protein is suddenly disassembled from the endocytic site. When the membrane tube undergoes scission, there is no more tubular curvature for the Rvs to bind to. The sharp decay is therefore consistent with a BAR scaffold that breaks upon vesicle scission because there is no more membrane interaction, releasing all the membrane-bound protein at once. A similar decay in the 4xd strain suggests that all the Rvs in this case is also bound to the membrane: if the protein was not bound to the membrane, fluorescent intensity would not decay sharply. Since the membrane is able to accommodate 1.4x the amount of BAR protein as the WT, it would suggest that at lower protein amounts, a tight helix that covers the entire tube is not likely. Adding molecules to a tube already completely covered by a scaffold would result in a change in Rvs assembly and disassembly dynamics. Further, additional molecules would have to be added at the top or base of a tight scaffold. At the top, the radius of curvature is decreased compared to the tube since this is the rounded vesicle region. At the base, the plasma membrane is nearly flat, and the Rvs BAR domain is similarly unlikely to favour interactions here. Otherwise the scaffold would have to be disrupted to add new molecules, which would likely slow down recruitment rate rather than speed it up. Molecules could also be added concentric to an existing scaffold. However, the concave surface of Rvs is known to interact with lipids, and multiple layers of BAR domains on the membrane tube would probably not show the sudden disassembly seen here. I assume that the membrane surface area does not change in the 4xd compared to 2xd from the identical movement of Sla1 in both cases (Fig.3.10A). It is possible that a wider tube is formed, which would increase the membrane surface area for BAR binding. This would, however, require the BAR domains to interact with a lower radius of curvature than in WT. This seems unlikely, and in the absence of any indication otherwise, I assume that the membrane tubes in all diploid and haploid cases have the same width. 4.2.2 A limit for how much Rvs can be recruited to the membrane In the case of Rvs duplication in haploids (2xh), a change in disas- sembly dynamics is seen (Fig.3.9C, Fig.4.3). In 2xh, the maximum number

of molecules recruited is 178±7.5 compared to the maximum of 113.505±5.2 in WT (1xh). This is means that nearly 1.6x the WT amount of protein is recruited to membrane tubes in in the 2xh case. The Rvs167 fluorescent intensity in 2xh shows a delay in disassembly. This suggests that the excess protein may not be directly on the mem- brane, since if the protein was membrane bound, when the membrane breaks, the protein must be released. The excess Rvs could either interact with the actin network via the SH3 domain, or interact with other Rvs dimers. By a similar argument as in 4.2.1 above, I do not expect that multiple layers of BAR domains are formed, and that the excess protein is recruited by the interaction of the SH3 domain. Another explanation for the delayed disassembly is that at high concentrations of Rvs like in the 2xh case, a tight BAR scaffold is formed, and the BAR domains interact with adjacent BAR domains. When the membrane undergoes scission, the protein is no longer membrane-bound, but lateral interactions delay disassembly of the scaffold. Lateral interactions between neighbouring BAR dimers have been shown in the case of Endophilin (Mim et al., 2012). It is not currently clear where the Rvs molecules are added in the 2xh case: supperresolution microscopy could clarify whether it is added at the membrane tube. Whatever the arrangement of the Rvs complex on the membrane, disassembly dynamics is changed in the case of 2xh, compared to the other haploid and diploid strains. Since the number of Rvs molecules is highest in this strain, this suggests that there is a limit to how much Rvs can assemble on the tube without altering interaction with the endocytic protein network. 4.2.3 Conclusions for Rvs localization All of these data support the idea that Rvs recruitment rate and total numbers are determined by concentration of protein in the cell. The maximum number of molecules that can interact with the membrane is limited by the surface area of the invagination. Although more can be recruited, Rvs molecules over a certain threshold interact in a different way with endocytic sites, possibly via the SH3 domain. Timing of recruitment to sites is by curvature-recognition via the BAR domain, while efficiency of recruitment and interaction with the actin network is established via the SH3 domain. 4.3 What causes membrane scission?

Rvs acts as a membrane scaffold preventing membrane scission

Invaginations in *rvs167*Δ cells undergo scission at short invagination lengths of about 80nm (Fig.3.2), compared to the WT lengths of 140nm. This shows that first, enough forces are generated at 80nm to cause scission. Then, that Rvs167 is required at membrane tubes to prevent premature scission. Prevention of scission at short invagination lengths can be explained by Rvs stabilizing the membrane invagination via membrane interactions of the BAR domain (Boucrot et al., 2012; Dmitrieff and Nedelec, 2015). Rvs preventing membrane scission could also be explained by the SH3 domain mediating actin forces to the invagination neck: one can imagine that the SH3 domain somehow decouples actin forces from the neck, and that this delays scission. Since invagination lengths of *rvs167*Δ cells are increased towards WT by overexpression of the BAR domain alone (Fig.3.12A), I propose that localization of Rvs BAR domains to the membrane tube stabilizes the membrane. This allows deep invaginations to grow until actin polymerization produces enough forces to overcome this stabilization and sever the membrane. Stabilization of the membrane tube increases with increasing amounts of BAR domains recruited to the membrane tube (Fig.3.12). The requirement for Rvs scaffolding cannot be removed by reducing turgor pressure (Fig.3.13), suggesting that the function of the scaffold is not to counter turgor pressure.

Scission efficiency decreases with decreased amounts of Rvs: in diploids, lowering the amount of Rvs by 20 molecules decreases scission efficiency to about 90% from 97%. This indicates that a particular coverage of the membrane tube is required for effective scaffolding by BAR domains. In support of this, in BAR strains, fewer numbers of Rvs are recruited, and scission efficiency is similarly reduced. At low concentrations of Rvs like in the 1xd cells, it is likeley that some membrane tubes recruit the critical number of Rvs, in which case the invaginations grow to near WT lengths. Over a certain amount of Rvs, adding more BAR domains does not increase the stability of the tube: in 4xd, the same amount of actin is recruited before scission as in the 2xd and 1xd strains. If

enough forces are generated at 80nm, why is scission efficiency decreased in *rvs167*Δ compared to WT? Forces from actin may be at a threshold when the invagination is at 80nm. There could be enough force to sever the membrane, but not enough to sever reliably. The Rvs scaffold then keeps the network growing to accumulate enough actin to reliably cause scission. Controlling membrane tube length could also be a way for the cell to control the size of the vesicles formed, and therefore the amount of cargo packed into the vesicle.

What causes membrane scission?

We have tested several scission models that include a major role for the Rvs complex. The seemingly obvious solution to the scission problem is the action of a dynamin-like GTPase. If loss of the yeast Dynamin Vps1 prevented or delayed scission, the membrane would continue to invaginate longer than WT lengths, and Sla1 movements of over 140nm should be observed. Rvs centroid movement would likely also be affected: a bigger jump inwards could indicate that a longer membrane has been cut. That neither is seen in the behaviour of coat and scission markers indicates that even if Vps1 is recruited to endocytic sites, it is not necessary for Rvs localization or function, and is not necessary for scission. The Inp51, Inp52 data tests the lipid hydrolysis model, in which synaptojanins hydrolyze PIP2 molecules that are not covered by BAR domains, resulting in a boundary between hydrolyzed and non- hydroplyzed PIP2. This model predicts that interfacial forces generated at the lipid boundary causes scission (Liu et al., 2006). Inp51 is not seen in patches at the cellular cortex, but this could be because protein recruitment is below our detection threshold. Inp52 localizes to the top of invaginations right before scission, consistent with a role in vesicle formation (Fig.3.7D). Some predictions of the lipid hydrolysis model are inconsistent with our data, however. First, vesicle scission is expected to occur at the interphase of the hydrolyzed and non-hydrolyzed lipid. Since the BAR scaffold covers the membrane tube, this interphase would be at the top of the area covered by Rvs. Kukulski et al., 2012 have shown that vesicles undergo scission at 1/3 the invagination length from the base: that is, vesicles generated by the lipid boundary would be smaller than have been measured. Second, removing forces generated by lipid hydrolysis by deleting synaptojanins should increase invagination lengths, since scission would be delayed or it would fail without those forces. Deletion of neither Inp51 nor Inp52 changes the invagination lengths: Sla1 movement does not increase. That the position of the vesicle formed is also unchanged compared to WT is indicated by the similar magnitude of the jump into the cytoplasm of the Rvs centroid. There are some changes in the synaptojanin deletion strains (Fig.3.8). In *inp51*Δ cells, Rvs assembly is slightly slower than that in WT. Therefore, Inp51 could play a role in Rvs recruitment. In the *inp52*Δ strain, about 12% of Sla1-GFP tracks retract, indicated that scission fails in those cases. Although this is low compared to the failed scission rate of *rvs167*Δ cells (close to 30%), this data could suggest a moderate influence of Inp52 on scission. Rvs centroid persists after scission for about a second longer in *inp52*Δ cells than in WT, indicating that disassembly of Rvs on the base of the newly formed vesicle is delayed. Inp52 is likely involved in vesicle un- coating Deletion of synaptojanin-like Inp52 does not affect the movement of the invagination. In spite of this, Sla1 patches persist for longer after scission in the *inp52*Δ than in WT cells, as does Rvs167, indicated by the arrows in Fig.3.8A,D. Persistence of both suggests that rather than the scission timepoint, post-scission disassembly of proteins from the vesicle is inhibited in *inp52*Δ cells. Inp52 then plays a role in recycling endocytic proteins from the vesicle to the plasma membrane. The slower assembly of Rvs in *inp51*Δ and the increase in coat retraction rates of *inp52*Δ could indicate that there is a slight effect on Rvs recruitment, and that lipid hydrolysis could play a small role in scission.

Protein-friction mediated membrane scission proposes that BAR domains induce a frictional force on the membrane, causing scission. In Rvs duplicated haploid cells (2xh), adding up to 1.6x the WT (1xh) amount of Rvs to membrane tubes does not affect the length at which the membrane undergoes scission (Fig.3.9). If more BAR domains were added to the membrane tube, frictional force generated as the membrane is pulled under it should increase, and the membrane should

rupture faster. That is, membrane scission occurs as soon as WT forces are generated on the tube. Since BAR domains are added at a faster rate in the 2xh cells, these forces would be reached at shorter invagination lengths. In 2xh cells, WT amount of Rvs is recruited at about 1.8 seconds before maximum fluorescent intensity, but scission does not occur at this time. Instead, Rvs continues to accumulate, and the invagination continues to grow. In diploid strains, adding 1.4x the WT amount of Rvs in the 4x Rvs case also does not change length of membrane that undergoes scission. Therefore, protein friction due to Rvs does not appear to contribute significantly to membrane scission in yeast endocytosis.

Maximum amount of Abp1 measured in all the diploid strains is about 220 molecules (Fig.3.11). In this case, only one allele of Abp1 is fluorescently tagged, so half the amount of Abp1 recruited is measured. The maximum amount of Abp1 recruited is then double that measured, which is about 440±20 molecules (assuming equal expression and recruitment of tagged and untagged Abp1). In WT haploid cells, the maximum number of Abp1 measured is 460±20 molecules. That the same number of molecules of Abp1 is recruited in all cases before scission indicates that scission timing depends on the amount of Abp1, and hence, on the amount of actin recruited. This data is consistent with actin supplying the forces necessary for membrane scission. The membrane invagination continues until the "right" amount of actin is recruited. At this amount of actin, enough forces are generated to rupture the membrane. The amount of force necessary is determined by the physical properties of the membrane like membrane rigidity, tension, and proteins accumulated on the membrane (Dmitrieff and Needeelec, 2015). Vesicle scission releases membrane-bound Rvs, resulting in release of the SH3 along with BAR domains. Release of the SH3 domains could indicate to its binding partner in the actin network that vesicle scission has occurred, beginning disassembly of actin components. In BAR strains, a low amount of actin is recruited (Fig.3.4C). Although the absence of the SH3 domain severely perturbs the actin network, the mechanistic effect of this perturbation is unclear.

Model for membrane scission

I propose that Rvs is recruited to sites by two distinct mechanisms. SH3 domains cluster Rvs at endocytic sites. This SH3 interaction increases the efficiency with which the BAR domains sense curvature on tubular membranes. BAR domains bind to endocytic sites by sensing tubular membrane. BAR domains are recruited over the entire membrane tube, but do not form a tight helical scaffold. Membrane shape is stabilized against fluctuations that could cause scission by the BAR-membrane interaction. This prevent actin forces from rupturing the membrane, and the invaginations continue to grow in length as actin continues to polymerize. BAR recruitment to membrane tubes is restricted by the surface area of the tube: after a certain amount of Rvs, the excess interacts with endocytic sites via the SH3 domain. Adding over a certain amount of Rvs also does not increase the stabilization effect on the tube. As actin continues to polymerize, at a certain amount of actin, enough forces are generated to overcome the resistance to membrane scission provided by the BAR scaffold. The membrane ruptures, and vesicles are formed. Synaptojanins may help recruit Rvs at endocytic sites: Inp51 and Inp52 have proline rich regions that could act as binding sites for Rvs167 SH3 domains. They are involved in vesicle uncoating post-scission, likely by dephosphorylating PIP2 and inducing disassembly of PIP2-binding endocytic proteins. Eventually phosphorylation regulation allows endocytic proteins to be reused at endocytic sites, while the vesicle is transported elsewhere into the cell.

Morbi luctus, wisi viverra faucibus pretium, nibh est placerat odio, nec commodo wisi enim eget quam. Quisque libero justo, consectetuer a, feugiat vitae, porttitor eu, libero. Suspendisse sed mauris vitae elit sollicitudin malesuada. Maecenas ultricies eros sit amet ante. Ut venenatis velit. Maecenas sed mi eget dui varius euismod. Phasellus aliquet volutpat odio. Vestibulum ante ipsum primis in faucibus orci luctus et ultrices posuere cubilia Curae; Pellentesque sit amet pede ac sem eleifend consectetuer. Nullam elementum, urna vel imperdiet sodales, elit ipsum pharetra ligula, ac pretium ante justo a nulla. Curabitur tristique arcu eu metus. Vestibulum lectus. Proin mauris.

Proin eu nunc eu urna hendrerit faucibus. Aliquam auctor, pede consequat laoreet varius, eros tellus scelerisque quam, pellentesque hendrerit ipsum dolor sed augue. Nulla nec lacus.

Methods and Materials

Guidelines can be included for standard research article sections, such as this one.

Nulla malesuada porttitor diam. Donec felis erat, congue non, volutpat at, tincidunt tristique, libero. Vivamus viverra fermentum felis. Donec nonummy pellentesque ante. Phasellus adipiscing semper elit. Proin fermentum massa ac quam. Sed diam turpis, molestie vitae, placerat a, molestie nec, leo. Maecenas lacinia. Nam ipsum ligula, eleifend at, accumsan nec, suscipit a, ipsum. Morbi blandit ligula feugiat magna. Nunc eleifend consequat lorem. Sed lacinia nulla vitae enim. Pellentesque tincidunt purus vel magna. Integer non enim. Praesent euismod nunc eu purus. Donec bibendum quam in tellus. Nullam cursus pulvinar lectus. Donec et mi. Nam vulputate metus eu enim. Vestibulum pellentesque felis eu massa.

Citations

LaTeX formats citations and references automatically using the bibliography records in your .bib file, which you can edit via the project menu. Use the `\cite` command for an inline citation, like **?**, and the `\citep` command for a citation in parentheses (**?**). The LaTeX template uses a slightly-modified Vancouver bibliography style. If your manuscript is accepted, the eLife production team will re-format the references into the final published form. *It is not necessary to attempt to format the reference list yourself to mirror the final published form.* Please also remember to **delete the line** `\nocite{*}` in the template just before `\bibliography{...}`; otherwise *all* entries from your .bib file will be listed!

Acknowledgments

Additional information can be given in the template, such as to not include funder information in the acknowledgments section.

References

Bensen, E. S., Costaguta, G., and Payne, G. S. (2000). Synthetic genetic interactions with temperature-sensitive clathrin in Saccharomyces cerevisiae. Roles for synaptojanin-like Inp53p and dynamin-related Vps1p in clathrin-dependent protein sorting at the trans-Golgi network. *Genetics*, 154(1):83–97.

Bitsikas, V., Corrêa, I. R., and Nichols, B. J. (2014). Clathrin-independent pathways do not contribute significantly to endocytic flux. *eLife*, 3:e03970.

Bui, H. T., Karren, M. A., Bhar, D., and Shaw, J. M. (2012). A novel motif in the yeast mitochondrial dynamin Dnm1 is essential for adaptor binding and membrane recruitment. *The Journal of cell biology*, 199(4):613–22.

Cestra, G., Castagnoli, L., Dente, L., Minenkova, O., Petrelli, A., Migone, N., Hoffmüller, U., Schneider-Mergener, J., and Cesareni, G. (1999). The SH3 domains of endophilin and amphiphysin bind to the proline-rich region of synaptojanin 1 at distinct sites that display an unconventional binding specificity. *The Journal of biological chemistry*, 274(45):32001–7.

Colwill, K., Field, D., Moore, L., Friesen, J., and Andrews, B. (1999). In Vivo Analysis of the Domains of Yeast Rvs167p Suggests Rvs167p Function Is Mediated Through Multiple Protein Interactions. *Genetics*, 152(3):881–893.

D'Hondt, K., Heese-Peck, A., and Riezman, H. (2000). Protein and Lipid Requirements for Endocytosis. *Annual Review of Genetics*, 34(1):255–295.

Farsad, K., Ringstad, N., Takei, K., Floyd, S. R., Rose, K., and De Camilli, P. (2001). Generation of high curvature membranes mediated by direct endophilin bilayer interactions. *The Journal of Cell Biology*, 155(2):193–200.

Ferguson, S. M., Brasnjo, G., Hayashi, M., Wölfel, M., Collesi, C., Giovedi, S., Raimondi, A., Gong, L. W., Ariel, P., Paradise, S., O'Toole, E., Flavell, R., Cremona, O., Miesenböck, G., Ryan, T. A., and De Camilli, P. (2007). A selective activity-dependent requirement for dynamin 1 in synaptic vesicle endocytosis. *Science*, 316(5824):570–574.

Ferguson, S. M., Raimondi, A., Paradise, S., Shen, H., Mesaki, K., Ferguson, A., Destaing, O., Ko, G., Takasaki, J., Cremona, O., O' Toole, E., and De Camilli, P. (2009). Coordinated actions of actin and BAR proteins upstream of dynamin at endocytic clathrin-coated pits. *Developmental cell*, 17(6):811–822.

Friesen, H., Humphries, C., Ho, Y., Schub, O., Colwill, K., and Andrews, B. (2006). Characterization of the Yeast Amphiphysins Rvs161p and Rvs167p Reveals Roles for the Rvs Heterodimer In Vivo. *Molecular Biology of the Cell*, 17(3):1306–1321.

Galli, V., Sebastian, R., Moutel, S., Ecard, J., Perez, F., and Roux, A. (2017). Uncoupling of dynamin polymerization and GTPase activity revealed by the conformation-specific nanobody dynab. *eLife*, 6:e25197.

Goud Gadila, S. K., Williams, M., Saimani, U., Delgado Cruz, M., Makaraci, P., Woodman, S., Short, J. C., McDermott, H., and Kim, K. (2017). Yeast dynamin Vps1 associates with clathrin to facilitate vesicular trafficking and controls Golgi homeostasis. *European Journal of Cell Biology*, 96(2):182–197.

Grabs, D., Slepnev, V. I., Songyang, Z., David, C., Lynch, M., Cantley, L. C., and De Camilli, P. (1997). The SH3 domain of amphiphysin binds the proline-rich domain of dynamin at a single site that defines a new SH3 binding consensus sequence. *The Journal of biological chemistry*, 272(20):13419–25.

Grigliatti, T. A., Hall, L., Rosenbluth, R., and Suzuki, D. T. (1973). Temperature-Sensitive Mutations in Drosophila melanogaster XIV. A Selection of Immobile Adults *. *Molec. gen. Genet*, 120:107–114.

Hoepfner, D., van den Berg, M., Philippsen, P., Tabak, H. F., and Hettema, E. H. (2001). A role for Vps1p, actin, and the Myo2p motor in peroxisome abundance and inheritance in Saccharomyces cerevisiae. *The Journal of Cell Biology*, 155(6):979–990.

Kaksonen, M. and Roux, A. (2018). Mechanisms of clathrin-mediated endocytosis.

Kaksonen, M., Sun, Y., and Drubin, D. G. (2003). A pathway for association of receptors, adaptors, and actin during endocytic internalization. *Cell*, 115(4):475–487.

Kaksonen, M., Toret, C. P., and Drubin, D. G. (2005). A modular design for the clathrin- and actin-mediated endocytosis machinery. *Cell*, 123(2):305–320.

Kishimoto, T., Sun, Y., Buser, C., Liu, J., Michelot, A., and Drubin, D. G. (2011). Determinants of endocytic membrane geometry, stability, and scission. *Proceedings of the National Academy of Sciences of the United States of America*, 108(44):E979–E988.

Kübler, E., Riezman, H., Riezman, H., and Riezman, H. (1993). Actin and fimbrin are required for the internalization step of endocytosis in yeast. *The EMBO journal*, 12(7):2855–62.

Kukulski, W., Schorb, M., Kaksonen, M., and Briggs, J. G. (2012). Plasma Membrane Reshaping during Endocytosis Is Revealed by Time-Resolved Electron Tomography. *Cell*, 150(3):508–520.

Lila, T. and Drubin, D. G. (1997). Evidence for physical and functional interactions among two Saccharomyces cerevisiae SH3 domain proteins, an adenylyl cyclase-associated protein and the actin cytoskeleton. *Molecular Biology of the Cell*, 8(2):367–385.

Liu, J., Sun, Y., Drubin, D. G., and Oster, G. F. (2009). The Mechanochemistry of Endocytosis. *PLoS Biol*, 7(9):e1000204.

Madania, A., Dumoulin, P., Grava, S., Kitamoto, H., Scharer-Brodbeck, C., Soulard, A., Moreau, V., and Winsor, B. (1999). The Saccharomyces cerevisiae Homologue of Human Wiskott-Aldrich Syndrome Protein Las17p Interacts with the Arp2/3 Complex. *Molecular Biology of the Cell*, 10(10):3521–3538.

Meinecke, M., Boucrot, E., Camdere, G., Hon, W.-C., Mittal, R., and McMahon, H. T. (2013). Cooperative recruitment of dynamin and BIN/amphiphysin/Rvs (BAR) domain-containing proteins leads to GTP-dependent membrane scission. *The Journal of biological chemistry*, 288(9):6651–61.

Moustaq, L., Smaczynska-de Rooij, I. I., Palmer, S. E., Marklew, C. J., and Ayscough, K. R. (2016). Insights into dynamin-associated disorders through analysis of equivalent mutations in the yeast dynamin Vps1. *Microbial cell (Graz, Austria)*, 3(4):147–158.

Munn, A. L., Stevenson, B. J., Geli, M. I., and Riezman, H. (1995). end5, end6, and end7: Mutations that cause actin delocalization and block the internalization step of endocytosis in Saccharomyces cerevisiae. *Molecular Biology of the Cell*, 6(12):1721–1742.

633 Nannapaneni, S., Wang, D., Jain, S., Schroeder, B., Highfill, C., Reustle, L., Pittsley, D., Maysent, A., Moulder, S.,
634 McDowell, R., and Kim, K. (2010). The yeast dynamin-like protein Vps1:vps1 mutations perturb the internal-
635 ization and the motility of endocytic vesicles and endosomes via disorganization of the actin cytoskeleton.
636 *European Journal of Cell Biology*, 89(7):499–508.

637 Peters, C., Baars, T. L., Bühler, S., and Mayer, A. (2004). Mutual control of membrane fission and fusion proteins.
638 *Cell*, 119(5):667–78.

639 Picco, A., Mund, M., Ries, J., Nédélec, F., and Kaksonen, M. (2015). Visualizing the functional architecture of the
640 endocytic machinery. *eLife*, page e04535.

641 Rooij, I. I. S.-d., Allwood, E. G., Aghamohammadzadeh, S., Hettema, E. H., Goldberg, M. W., and Ayscough,
642 K. R. (2010). A role for the dynamin-like protein Vps1 during endocytosis in yeast. *Journal of Cell Science*,
643 123(20):3496–3506.

644 Rothman, J. H., Raymond, C. K., Gilbert, T., O'Hara, P. J., and Stevens, T. H. (1990). A putative GTP binding protein
645 homologous to interferon-inducible Mx proteins performs an essential function in yeast protein sorting. *Cell*,
646 61(6):1063–1074.

647 Rothman, J. I. and Stevens, T. H. (1986). Protein Sorting in Yeast: Mutants Defective in Vacuole Biogenesis
648 Mislocalize Vacuolar Proteins into the Late Secretory Pathway. Technical report.

649 Shupliakov, O., Löw, P., Grabs, D., Gad, H., Chen, H., David, C., Takei, K., De Camilli, P., and Brodin, L. (1997).
650 Synaptic vesicle endocytosis impaired by disruption of dynamin-SH3 domain interactions. *Science (New York,*
651 *N.Y.)*, 276(5310):259–63.

652 Simunovic, M., Manneville, J.-B., Renard, H.-F. O., Johannes, L., Bassereau, P., Callan, A., Correspondence, J.,
653 Evergren, E., Raghunathan, K., Bhatia, D., Kenworthy, A. K., Voth, G. A., Prost, J., Mcmahon, H. T., and Callan-
654 Jones, A. (2017). Friction Mediates Scission of Tubular Membranes Scaffolded by BAR Proteins. *Cell*, 170:1–13.

655 Sivadon, P., Crouzet, M., and Aigle, M. (1997). Functional assessment of the yeast Rvs161 and Rvs167 protein
656 domains. *FEBS letters*, 417(1):21–27.

657 Skruzny, M., Brach, T., Ciuffa, R., Rybina, S., Wachsmuth, M., and Kaksonen, M. (2012). Molecular basis for
658 coupling the plasma membrane to the actin cytoskeleton during clathrin-mediated endocytosis. *Proceedings*
659 *of the National Academy of Sciences of the United States of America*, 109(38):E2533–42.

660 Smaczynska-de Rooij, I. I., Allwood, E. G., Mishra, R., Booth, W. I., Aghamohammadzadeh, S., Goldberg, M. W., and
661 Ayscough, K. R. (2012). Yeast Dynamin Vps1 and Amphiphysin Rvs167 Function Together During Endocytosis.
662 *Traffic*, 13(2):317–328.

663 Sweitzer, S. M. and Hinshaw, J. E. (1998). Dynamin Undergoes a GTP-Dependent Conformational Change Causing
664 Vesiculation. *Cell*, 93(6):1021–1029.

665 Takei, K., McPherson, P. S., Schmid, S. L., and Camilli, P. D. (1995). Tubular membrane invaginations coated by
666 dynamin rings are induced by GTP-γS in nerve terminals. *Nature*, 374(6518):186–190.

667 Youn, J.-Y., Friesen, H., Kishimoto, T., Henne, W. M., Kurat, C. F., Ye, W., Ceccarelli, D. F., Sicheri, F., Kohlwein, S. D.,
668 McMahon, H. T., and Andrews, B. J. (2010). Dissecting BAR Domain Function in the Yeast Amphiphysins Rvs161
669 and Rvs167 during Endocytosis. *Molecular Biology of the Cell*, 21(17):3054–3069.

670 Yu, X. and Cai, M. (2004). The yeast dynamin-related GTPase Vps1p functions in the organization of the actin
671 cytoskeleton via interaction with Sla1p. *Journal of Cell Science*, 117(17):3839–3853.

672 Zhang, P. and Hinshaw, J. E. (2001). Three-dimensional reconstruction of dynamin in the constricted state. *Nature*
673 *Cell Biology*, 3(10):922–926.

674 Zhao, W.-D., Hamid, E., Shin, W., Wen, P. J., Krystofiak, E. S., Villarreal, S. A., Chiang, H.-C., Kachar, B., and Wu, L.-G.
675 (2016). Hemi-fused structure mediates and controls fusion and fission in live cells. *Nature*, 534(7608):548–52.